Proceedings of the 20th International Conference on Soil Mechanics and Geotechnical Engineering– Rahman and Jaksa (Eds)

Improvement of railway trackbeds using geogrids - field tests and monitoring

Amélioration des plateformes ferroviaires par géogrilles - essais en voie et instrumentation

Olatounde Yaba, Jean-François Ferellec, Amine Dhemaied & Quôc Trung Pham
DGII-VA-CIR, SNCF Réseau, France, olatounde.yaba@reseau.sncf.fr

Fabrice Emeriault & Orianne Jenck
Laboratoire 3SR, Univ. Grenoble Alpes, France

ABSTRACT: Faced with increasingly demanding maintenance challenges, SNCF Réseau proposes to use geogrids to improve trackbeds (interlayer or subballast with capping layer) during renovations on its conventional rail lines (speed limit ≤ 220km/h). Currently, knowledge on the mechanical behaviour of geogrid stabilised subballast is limited, especially in the context of the French National Rail Network. Hence the interest in setting up an experiment to quantify the improvements brought by subballast stabilising geogrids in operating conditions. This paper presents the renovation, instrumentation and monitoring of a conventional track section equipped with two instrumented geogrids. The instrumentation allows continuous dynamic measurement of soil stresses (above and below the geogrids) and of geogrid strains. Preliminary results confirm that the system is working properly, but do not provide enough hindsight to draw any conclusions concerning the geogrids' effectiveness. The continued analysis of the monitoring results over the next several years will make help establish benchmarks to decide whether this is a relevant application for geogrids, and to differentiate the performance of several types of geogrids.

RÉSUMÉ : Face au besoin de renouveler les structures d'assises (ballast, couche intermédiaire ou sous-couche et couche de forme) des lignes classiques (circulées à moins de 220km/h) et confronté à des enjeux de plus en plus contraignants, SNCF Réseau propose d'utiliser des géogrilles dans les couches sous ballast (sous-couche/couche de forme). A l'heure actuelle, les connaissances sur le comportement mécanique des couches sous ballasts améliorées par géogrilles sont limitées, surtout dans le contexte du Réseau Ferré National Français. D'où l'intérêt de mettre en place des expérimentations en conditions opérationnelles, pour quantifier les apports de géogrilles dans ces couches. Cette communication présente le renouvellement, l'instrumentation et le suivi d'un tronçon de ligne classique équipée de deux géogrilles instrumentées. L'instrumentation permet la mesure dynamique et continue des contraintes dans le sol et des déformations des géogrilles. Les résultats préliminaires permettent de confirmer le bon fonctionnement du système d'instrumentation, ils fourniront dans quelques mois suffisamment de recul pour tirer des conclusions sur l'apport des géogrilles. L'analyse à long-terme permettra de statuer sur la pertinence de l'utilisation de géogrilles pour cette application et sur les performances des différentes géogrilles.

KEYWORDS: geogrid, subballast, monitoring, railways.

1 INTRODUCTION

The increase of traffic imposes large cyclic loads on railway trackbeds (interlayer or subballast with capping layer), which contribute to the appearance of geometry defects on the tracks. This phenomenon is particularly remarkable on French conventional rail lines (speed limit ≤ 220km/h) and can impact train safety as well as passenger comfort. Thus, SNCF has undertaken major efforts to find a cost-effective remedy. The use of geosynthetics, particularly geogrids, in the subballast layer represents one such remedy. When placed at the interface of granular soils, geogrids (that have apertures of various sizes and shapes) could improve the mechanical properties of these soils by interlocking the grains in their apertures (Carroll, 1988).

At present, knowledge of the mechanical behaviour of geogrids and their contribution to subballast layers in field conditions is limited, especially in the context of the French National Rail Network (NRN). Most available field studies have focused on geogrids placed in the ballast layer. These studies have shown the effectiveness of geogrids in reducing ballast wear and lateral spreading (Horníček et al., 2017; Nimbalkar & Indraratna, 2016; Lenart & Klompmaker, 2014; Fernandes et al., 2008; Sharpe et al., 2006). Nevertheless, they do not allow one to draw satisfactory conclusions regarding the likeliness of similar improvements in subballast. Also, the use of geogrids in the ballast layer or directly underneath it is not compatible with current practices on the NRN (maintenance techniques such as tamping, traffic, etc.). Hence the interest in setting up a field experiment to directly quantify the improvements brought by subballast stabilising geogrids in operating conditions on the NRN.

This paper presents the renewal, instrumentation and monitoring of a conventional track section which is equipped with two instrumented geogrids. The setup, which is capable of sampling at a rate of 2000Hz, allows for 1) the detection and measurement of the axle loads of oncoming trains, 2) the measurement of lateral strains in the geogrids, and 3) the measurement of the stresses applied in the trackbed above and below the geogrids. The experiment is designed to run for ten years, at least. As of the writing of this paper, only six months of data are available.

2 SITE INTRUMENTATION

2.1 *Context and initial considerations*

The site is located on a line of the Bourgogne-Franche-Comté regional rail network, which receives daily traffic of 3,500 to 7,000 equivalent tonnes from trains circulating at a maximum speed of 120km/h. It was instrumented in conjunction with some modernisation of the rail line during the first semester of 2020.

Preliminary design studies highlighted the presence of drainage problems and a low strength subgrade in several locations along the line, which lead to mud pumping under traffic loads. Renovating the superstructure (ballast and sleepers) without renewing the trackbed (the intermediate layer in this case) could have worsened this situation. Thus, the design team proposed to excavate up to 35cm below the ballast layer, then lay a separation/filtration geotextile, a geogrid and 35cm of unbound aggregate (the subballast, with grain size of 0-31.5mm). This provided an excellent opportunity to monitor one of these problematic locations. More precisely, the instrumented site

comprises a 40-metre stretch that runs along the platform of a small train station. This train station was chosen because fifteen to twenty trains run through the station each day, but only one stops. Thus, the site provides a good sample of fast-moving trains for dynamic measurements, while being easy to access and benefitting from the availability of a stable power supply.

The subgrade (in situ soil) consists of silty-sand with pockets of alluvial gravel (rolled gravel). Plate load tests were performed on the exposed subgrade using a light weight deflectometer (Minidyn™). They confirmed that the subgrade is of low strength. Of the 60 tests performed, immediately after excavation, 45 measured an Ev2 modulus of less than 30MPa, which means that the subgrade is "in its current state unfit to support any track structure" according to SNCF's standards. One can see in Figure 1 that there are several abnormally high values (> 30MPa), especially in the top part of the figure (left-hand side of the site); they result from the presence of gravel pockets. Excluding these values, the average Ev2 modulus is 23.92MPa with a standard deviation of 4.75MPa.

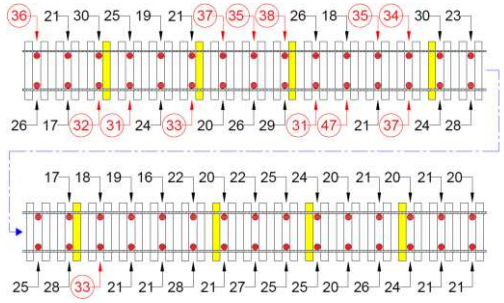

Figure 1. Subsoil deformation moduli in MPa along the site. The distance between the axes of each sleeper is 60cm. Note that the site consists of one continuous track. It was broken into two halves to facilitate the visual representation.

Note that the Minidyn™ has a 30cm diameter plate, transfers 98.1J to the ground with each impact and is capable of measuring moduli from 10 to 80MPa (Rincent ND Technologies, 2017).

2.2 *Instrumentation configuration*

The instrumented site is divided into three zones (Figure 2). The zones at each extremity of the site (each 12.6m long) are equipped with geogrids (GGR1 and GGR2) while the zone in the middle (9.6m long) is left without a geogrid, for reference (REF). The lengths of these zones were chosen based of logistical constraint, while considering the fast that the load of a given axel is generally spread over five sleepers. Hence one would need a minimum of 1.5m on each side of an instrumented sleeper in order to ensure that it is not being influenced by adjacent zones.

Remember that a geotextile is laid directly on top of the subgrade along the full length of the site, including the reference zone. In total, there are eight instrumented sections, three for each of the geogrids (S1, S2 and S3) and two for the reference zone (REF_1 and REF_2).

Both geogrids are polypropylene punched and drawn triaxial grids with a hexagonal height of 80mm (Figure 3), and 100% junction efficiency (European Organisation for Technical Approvals, 2017). The only characteristics that differentiate the two geogrids are their radial secant stiffnesses. They are 480kN/m at 0.5% strain and 360kN/m at 2% strain for GGR1 and 360kN/m at 0.5% strain and 250kN/m at 2% strain for GGR2 (determined according to EOTA TR41). These two geogrids were selected to study the influence of a geogrid's stiffness on its performance, in a given set of conditions.

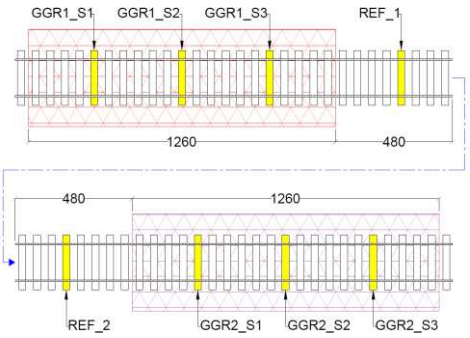

Figure 2. Site configuration with the position of each instrumented section (shaded sleepers). The distance between the axes of each sleeper is 60cm. Note that the site consists of one continuous track. It was broken into two halves to facilitate the visual representation.

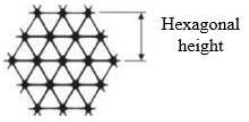

Figure 3. Hexagonal height of a geogrid with triangular apertures.

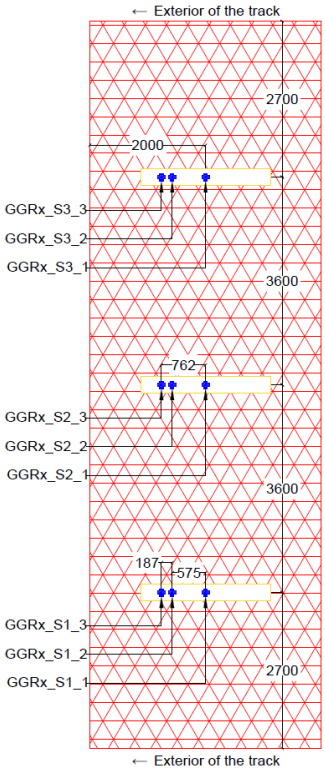

Figure 4. Strain gauge positions on each instrumented geogrid. The void rectangles represent the estimated positions of sleepers above the strain gauges.

Each geogrid is instrumented with nine strain gauges, bonded to transverse ribs, in order to record strain in the transversal direction. Figure 4 details the position of the gauges. For each instrumented section, the gauges are positioned: a) in the track's central axis, 762mm from each rail (GGRx_Sx_1); b) in an intermediate axis, 187mm from the outer rail (GGRx_Sx_2); c) beneath the axis of the outer rail (GGRx_Sx_3). The intermediate axis represents the position where one can expect a median stress relative to those applied under the rail and under the track's central axis at the depth of the geogrid, when loaded by a passing train.

Feedback from a previously instrumented site has revealed that temperature variations are responsible for most irreversible strains in this type of setup with this type of geogrid (Yaba et al., 2020). Thus, temperature sensors are places near each row of strain gauges between the geotextile and the geogrid. Temperature can be used to adjust for deviations that will eventually be observed in long-term strains measurements.

There are total pressure cells (290mm in diameter) buried 100 mm below and/or 200 mm above each geogrid (depending on the section). The total pressure cells are: a) absent in sections GGR1_S1 and GGR2_S3; b) present only under the geogrid in sections GGR1_S3 and GGR2_S1; c) and present above and below the geogrid in the other four sections (Figure 5).

All the sensors have been connected to a CRONOSflex data logger (from imc Test & Measurement GmbH) equipped with a modem and transmission system to allow remote monitoring. The setup continuously samples at a rate of 2000Hz and records data 1) each time a train is detected by sensors attached to the rails at each end of the site (dynamic measurement); 2) every hour, if no trains are detected on the site (static measurement). This allows one to observe and analyse both the transient and permanent states of the geogrid and trackbed over the long-term. The sensors that detect on-coming trains are composed of a full-bridge of strain gauges. They also measure axle loads using a proprietary algorithm developed by the SNCF Réseau track instrumentation division (DGII-VA-T3).

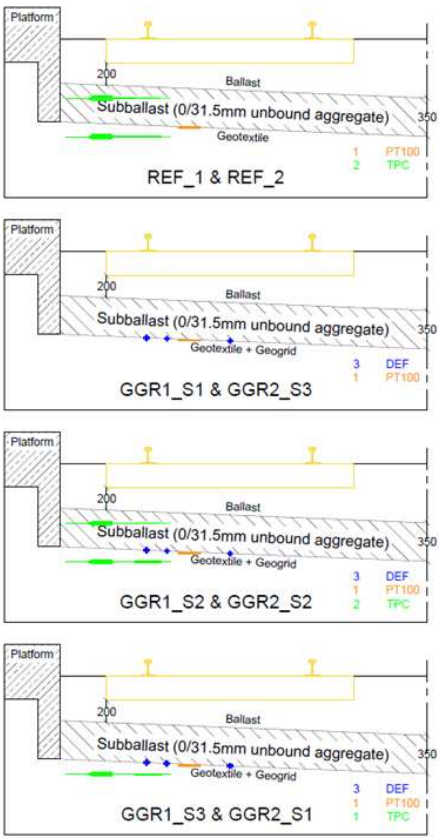

Figure 5. Instrumented cross-sections showing the positions of the strain gauges (crosses = DEF), the temperature sensors (small horizontal bars = PT100) and the total pressure cells (large horizontal bars = TPC).

The system was designed based on feedback from a previously instrumented site (Yaba et al., 2020) which was inspired by work done in Australia (Anantanasakul et al., 2012) and Slovenia (Lenart & Klompmaker, 2014). It will be supplemented by dynamic rail and sleeper deflection measurements (deflections when trains pass) at intervals of four to six months starting in July 2021 (if possible, considering the Covid19 pandemic). The specifications for each type of sensor are summarised in Table 1.

Table 1 : Sensors and their respective technical specifications

Sensor type	Stain gauge	Temperature sensor	Total pressure cell
Manufacturer	Kyowa	RS-Pro	Telemac
Name	KFGS-1N-120-C1-11 N15C2	PT100	TPC 229mm
Measurement range	±5%	-20 to +200°C	0 to 500kPa
Accuracy	0.02µm/m	±0.15°C	±1.25kPa
Resolution	0.001µm/m	0.01°C	0.05kPa
Temperature range	-196 to +150°C	-20 to +200°C	-50 to +150°C

2.3 *Installation methodology*

Work on the site consisted of: 1) removal of the ballast and the interlayer (excavation up to 55 cm below the lower face of the sleepers); 2) levelling the subgrade with a 4% slope towards the inside of the track (drainage located on the opposite track); 3) smoothing the exposed subgrade with a Bomag BW75H compactor; 4) measurement of the subgrade Ev2 modulus using the Minidyn™; 5) placement of a geotextile on the subgrade followed by the instrumented geogrids on the geotextile and verification of the alignment of the monitored sections; 6) laying 35cm of unbound aggregate (laid in two layers of 20cm and 15cm respectively) and compacting to a density of 97-100% of Modified Proctor's optimum; 7) installing the superstructure (ballast, sleepers and rail) and adding the finishing touches (tamping, dynamic stabilisation, etc.).

The instrumentation had to be integrated into the work described above. Thus, it was necessary to work closely and coordinate with SNCF's track instrumentation division, the maintenance team of Bourgogne-Franche-Comté regional rail network and the contractors to: 1) plan tasks starting six months before on-site work; 2) preinstall and prewire all the sensors then organise on-site delivery; 3) set up the datalogger during the removal of the existing superstructure; 4) perform the plate loading tests, dig trenches and bury sensors in the subgrade, during excavation; 5) properly position the instrumented geogrids; 6) properly route the cables to the data logger; 7) embed sensors in the unbound aggregate; 8) connect and test all the sensors as the work progressed; 9) install sensors for train detection and axle load measurements after tamping and dynamic stabilisation of the ballast. Note that each strain gauge was protected by a layer of resin sandwiched between two sheets of aluminium foil. This protection was designed (by a subcontractor) to have as little effect as possible on the overall strain measurements. The total pressure cells were each placed in beds of fine sand, to ensure proper stress distribution on their surfaces.

Most of the work was done in March 2020, except for the last stages which were done between May and August 2020 (due to interruptions caused by lockdowns and work restrictions during the early stages of the Covid19 pandemic). The first dynamic measurements were recorded in late August after the line reopened.

3 PRELIMINARY RESULTS

The following section summarizes the observations based on the results available from late August to late February 2021. The present data illustrates the dynamic behaviour at each passage of

a train. Feedback from previous sites has showed that long-term trends, notably for cumulative strain, are not noticeable over periods shorter than a year. Furthermore, they are strongly affected by seasonal variations in temperature (Yaba et al., 2020). Considering that the benefits of using geogrids are expected to become apparent over the long-term, the discussion will mostly be centred around the current state of the monitoring system and future possibilities.

Note that geotechnical convention is used. Thus, in all figures, positive values represent compression/contraction and negative values represent traction/extension. The data was processed using a python code which recovers raw data files from the CRONOSflex data logger, converts them into physical units (i.e. kN, µm/m, kPa…), filter the data signals using Butterworth filter (Ellis, 2012) and synchronises the signals such that each measurement can be linked to a specific bogie based on the peak stresses and strains.

3.1 *Trains and axle loads*

As of the writing of this paper, the system has logged more than six months of data. Most of the recordings correspond to the circulation of passenger trains travelling between 115 and 120km/h. The load profiles for the two most frequent types of train are shown in Figure 6. One can observe that the locomotive bogies (at the head and tail) of each train are heavier than those of the passenger cars (in the middle). These loads will be correlated with the other recorded data using big data analytics.

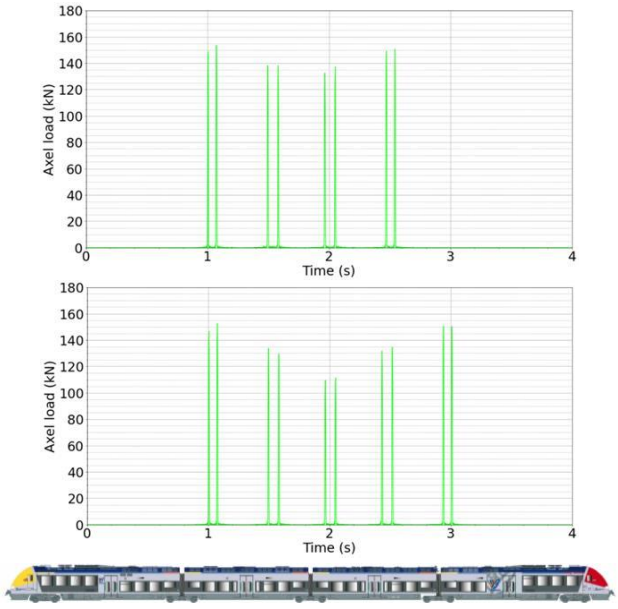

Figure 6. Axle load profile of 3 car (with 4 bogies, top) and 4 car (with 5 bogies, bottom) passenger trains circulating on the instrumented site. An image of a 4 car Bombardier B81500 is provided for reference.

3.2 *Strain measurements*

The first observation concerning the strain measurements is that the unfiltered signals have become significantly less noisy over time. Figure 7 illustrates this phenomenon, which can be attributed to the rearrangement of the grains in the subballast layer and their stabilisation due to interlocking in the geogrid. This may also be due to the water content of the trackbed. The first measurements were recorded after a significant dry spell, which could have hindered proper packing of the subballast thus amplifying dynamic effects. A reappearance of noise during the next dry season, would strengthen this hypothesis.

When looking at the full range of strains measured in all sections for a given train (Figure 8 and Figure 9), one can see that the magnitudes of the strains vary more significantly between different sections of the same geogrid than they do between the two geogrids in general (from 200 to 800µm/m). This seems to be due to the variation of the Ev2 modulus of the subgrade along the track coupled with the heterogeneity of the subballast material (which contains many large grains). For each geogrid, there are less strains in the sections located above stiffest areas with 38MPa for GGR1_S3 (see Ev2 modulus and strains on Figure 8) and 24 MPa for GGR2_S2 (see Ev2 modulus and strains on Figure 9).

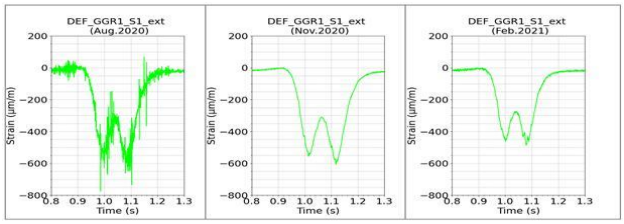

Figure 7. Strain due to equivalently loaded bogies at 3 month intervals on gauge DEF_GGR1_S1_3 (see Figure 2 & Figure 4 for positions). A similar phenomenon appears for most of the strain gauges.

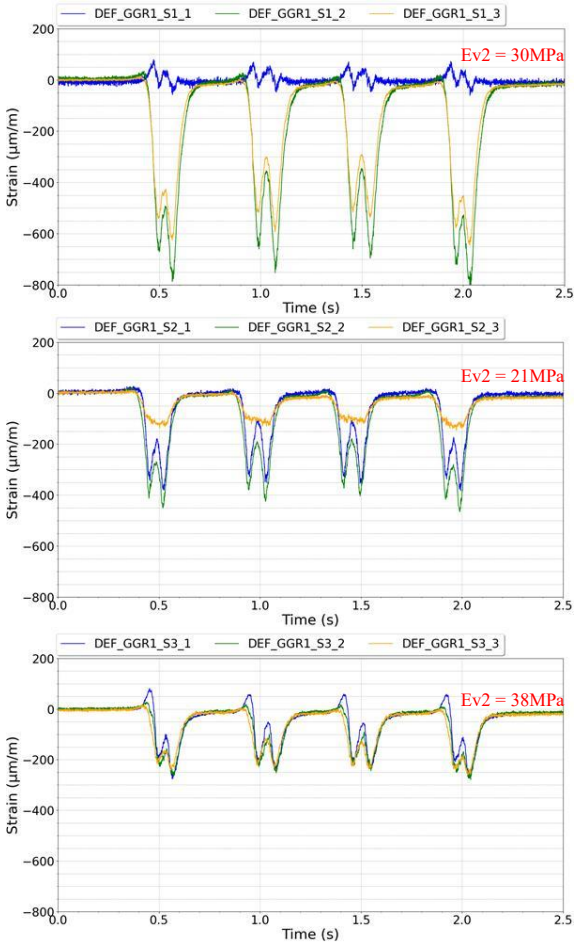

Figure 8. GGR1 strains across instrumented sections for a 3 car B81500 train moving from the top graph to the bottom graph. Note that each graph represents one of the sections labeled in Figure 2.

Note that there is a contraction in DEF_GGR1_S1_1. This section is near the transition from the old trackbed (with an interlayer) to the renewed trackbed (with a distinct subballast

layer). Considering this, the initial hypothesis was that the anomaly is most likely caused by a combination of dynamic effects due the transition. However, after several months of observation, it seems more likely that there is an improper interlocking of the subballast grains near the strain gauge or that the strain gauge is damaged. This strain measurement will probably be excluded from future analysis to avoid skewing the data.

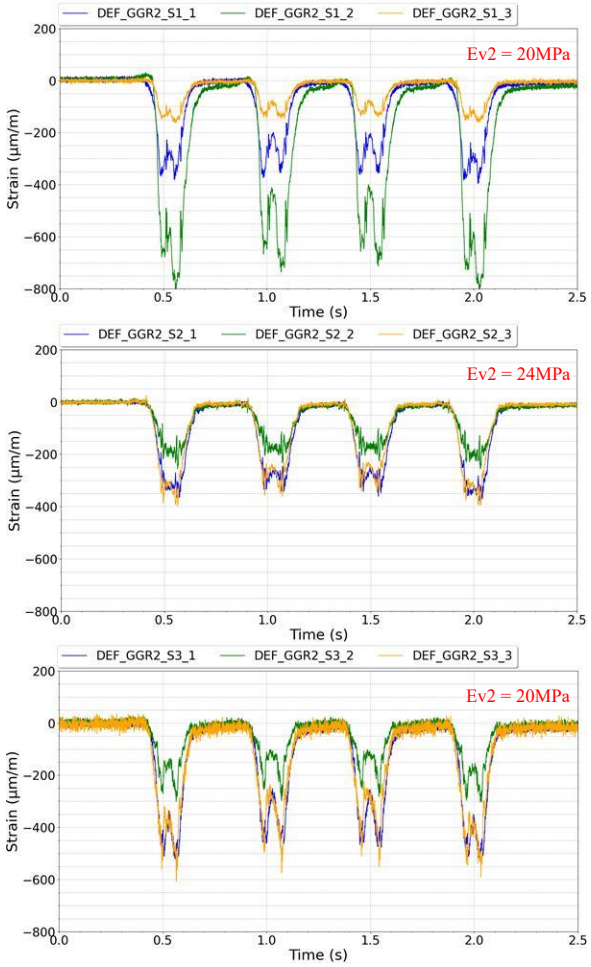

Figure 9. GGR2 strains across instrumented sections for a 3 car B81500 train moving from the top graph to the bottom graph. Note that each graph represents one of the sections labeled in Figure 2.

3.3 *Stress measurements*

The stress applied to the subballast and subgrade are presented in Figure 10. These stresses correspond to the train used for Figure 8 and Figure 9. Note that the stresses are specifically the surcharges applied by the train's axles, and that the signals are smoothed using the aforementioned Butterworth filter. This adjustment of the stress values simplifies the interpretations of the measurement and will facilitate statistical analysis.

A more interesting exercise consists in singling out a bogie and analysing its effect on each section where stresses are measured. On the following figures, the peaks correspond to a wheel load of approximately 75kN, which should produce a surcharge of 50 to 60kPa on the top layer of TPCs. The wheel load is used here because the total pressure cells are located directly below the outer rail, so they should mostly be affected by the outer wheel of the axle.

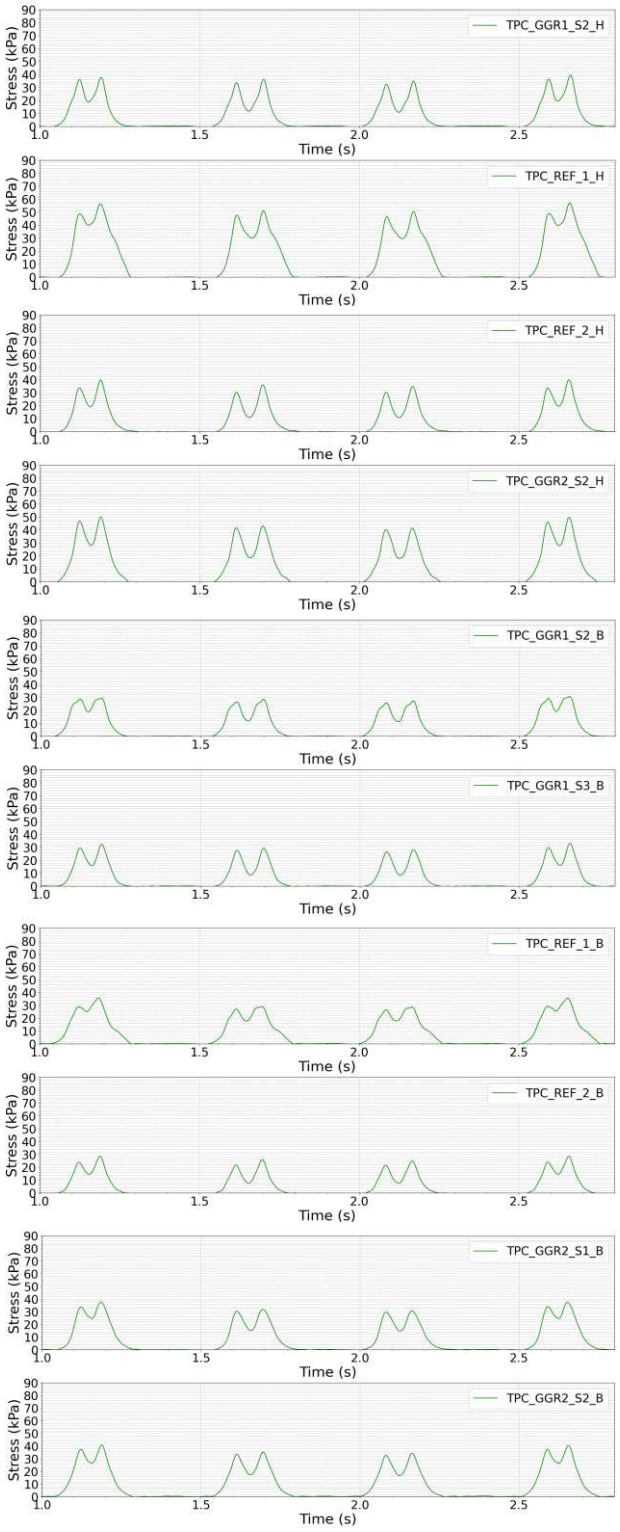

Figure 10. Stresses applied to the subballast (top, indexed _H) and subgrade (bottom, indexed _B) by a given train.

Focusing on the first bogie, the stress peaks have been aligned for each of the four points where there are total pressure cells both above and below the geogrid. These are illustrated in Figure 11 (data from late August 2020) and Figure 12 (data from late February 2021); un-smoothed signals are used to avoid bias in the visual representation. For now, there are no significant changes in the stress profiles. Long-term, we expect to see the profiles remain stable in the sections equipped with geogrids

(GGR1 and GGR2), while they degrade in the reference sections (REF_1 and REF_2). This is because the geogrids should keep the subballast above them nicely packed and stable relative to the control sections. Hence, reducing vertical stress and increasing lateral stress, by reducing lateral spreading.

Thus, it would not be surprising to see the stress curves in the subballast and the subgrade remain close to each other over the long-term in the geogrid stabilised sections. The opposite would be true for the stress curves in the reference sections, as the subballast spreads laterally. However, it may take several years for this to manifest because the trackbed is constrained by the train station's platform on one side.

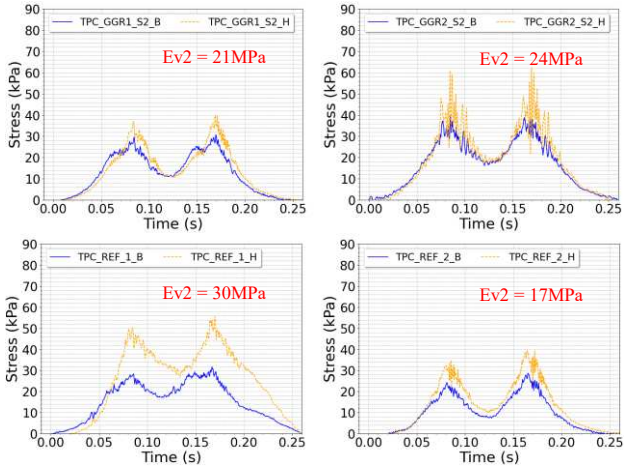

Figure 11. Comparison between stresses applied at GGR1 (top left), GGR2 (top right), REF_1 (bottom left) and REF_2 (bottom right), in the subgrade (solid lines) and the subballast (dotted line) by a single bogie with wheel loads of approximately 75kN. For a 3 car B81500 passing in late August 2020.

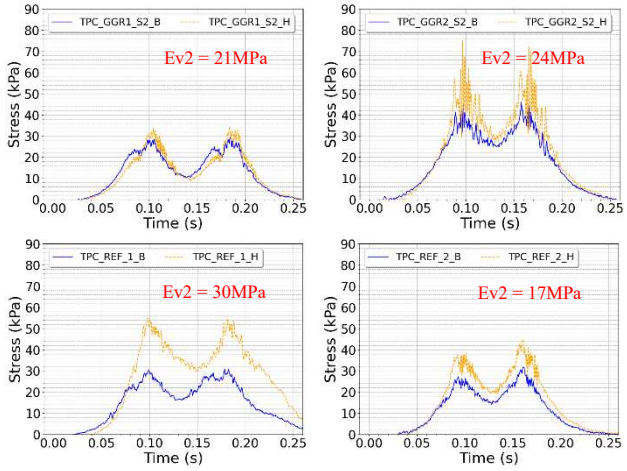

Figure 12. Comparison between stresses applied at GGR1 (top left), GGR2 (top right), REF_1 (bottom left) and REF_2 (bottom right), in the subgrade (solid lines) and the subballast (dotted line) by a single bogie with wheel loads of approximately 75kN. For a 3 car B81500 passing in late February 2021.

Looking at the figures above, one should note the difference in response between TPC_REF_1_H and TPC_REF_2_H. This is likely due to the difference of subgrade Ev2 modulus between the two sections. One should expect greater stress localisation in the stiffer parts of the subgrade, which is precisely what is observed.

To further compare the behaviour between the various zones, the ratio of stress measured in the subgrade relative to the stress measured in the subballast (transfer ratio, Eq. 1) was calculated using the peak stress measured for each train. This stress transfer ratio, for each zone, was then plotted against the corresponding axle loads (

Figure 13). Note that there are three distinct clusters on each graph; the two clusters with axle loads below 160kN are passenger trains and the rest are freight trains. The weighted averages (aka centroids) of the larger passenger cluster and the freight cluster are identified using triangular markers. There values are summarised in Table 2.

$$Transfer\ Ratio = TPC\_B\ /\ TPC\_H \quad (1)$$

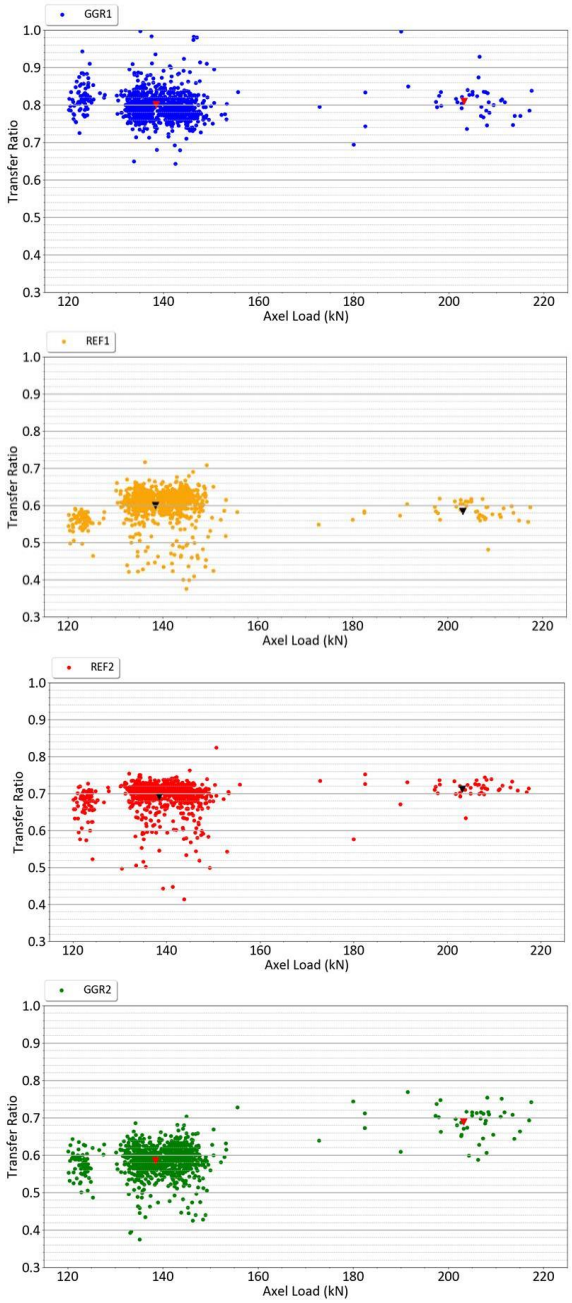

Figure 13. Stress transfer ratio from subballast to subgrade relative to axle load for each zone (GGR1, REF1, REF2 & GGR2; from top to bottom), with a marker for the weighted average of each cluster.

Overall, the transfer ratios for GGR1 validate expectations based on the mechanisms described by Perkins (1999), who stipulated that the confinement of the aggregate will result in a

reduction in the vertical stress above the geogrid. Thus leading to a higher value for the transfer ratio.

On the other hand, in terms of transfer ratio, GGR2 seems to behave like REF1 (which has the same subgrade Ev2 modulus). It is also interesting to note that, unlike the other zones, the transfer ratio for GGR2 is correlated to the axle load (see Table 2, for precise values). There seems to be a threshold above which GGR2 is mobilised, which would mean that it may not be useful in areas with mostly passenger trains. More analysis is required to determine relationship between the transfer ratio, the axle load and the subgrade Ev2 modulus (for each geogrid).

Table 2 : Values of transfer ratio centroids for each zone.

Zone	Passenger (~140kN)	Freight (~200kN)
GGR1	0.80	0.81
REF1	0.60	0.58
REF2	0.69	0.71
GGR2	0.58	0.69

The final step in comparing the different zones involves plotting the distribution of peak stresses measured in the subgrade at each point. Figure 14 shows this distribution for a sample of approximately 1000 trains. One can observe two important points. First, the modal values of peak stress overlap for the points below GGR1 and are quite distinct for the points below the other section; despite the greater variability of Ev2 modulus below GGR1. Second, the stresses follow a normal distribution; thus the first observation can be validated using a paired t-test.

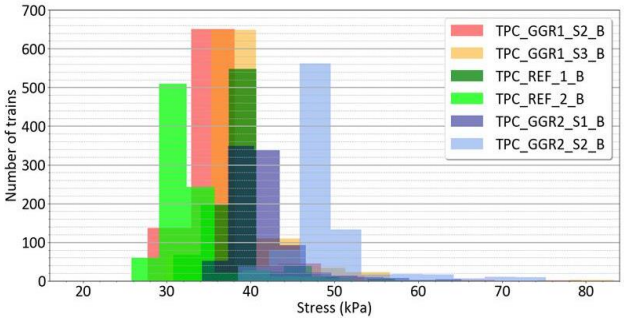

Figure 14. Comparison between the peak stresses applied in the subgrade at both points of measurement in each of the three zones (GGR1, REF and GGR2), for approximately 1000 trains.

The paired t-test is a statistical procedure used to determine whether the mean difference between two sets of observations is zero; i.e. the null hypothesis. In the present case, the pairs are the stress measurements for each monitored zone (GGR1, REF and GGR2). Thus the measurements from TPC_GGR1_S2_B were compared to those from TPC_GGR1_S3_B, and so on for each train included in the sample. These pairs are illustrated in Figure 15. Statistical significance is determined by calculating the p-value, which gives the probability of observing the test results under the null hypothesis. p-values greater than 0.050, 0.025 and 0.010 were used to validate the null hypothesis. A detailed explanation of the t-test and its procedure can be found in Applied Statistics and Probability for Engineers (Montgomery & Runger, 2018) or any other engineering statistics textbook.

The t-test was thus performed on each train in each zone. For each zone, if the two sets of stress measurements in the subgrade where statistically the same (i.e. the p-value is greater than the prescribed limit), then the null hypothesis was considered valid. The percentage of trains for which the null hypothesis was validated are summarised in Table 3.

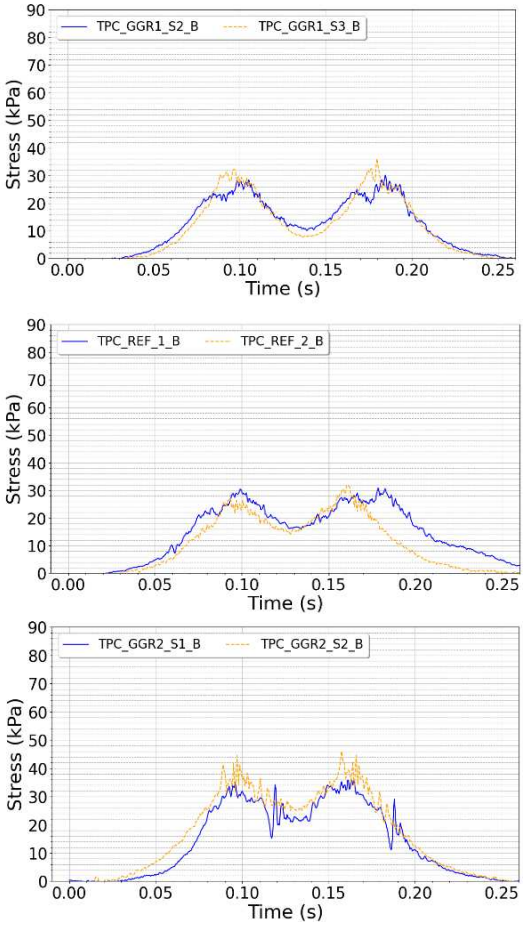

Figure 15. Example of the stress measurement pairs used in the t-test to verify whether the geogrids improve stress distribution in the trackbed.

Table 3 : Percentage of cases that verify the null hypothesis in each zone, for each p-value (i.e. percentage of cases with uniform load distribution)

Zone	p = 0.050	p= 0.025	p = 0.010
GGR1	22.51 %	25.83 %	30.81 %
GGR2	15.97 %	17.43 %	20.44 %
REF	3.84 %	4.57 %	5.39 %

The results show that no matter the p-value, the percentage of cases with a valid null hypothesis is highest for GGR1, followed by GGR2, then REF. This confirms that the geogrids improve the stress distribution. GGR1 (the stiffer geogrid) provides the best stress distribution and, despite previous fears, GGR2 provides a notable improvement as well.

Note that, even in the best-case scenario, the percentage of cases where the geogrids are shown to improve stress distribution is relatively low. This was expected because the test was performed without taking any of the many factors that could influence stress distribution into account (subgrade Ev2 modulus, water content, etc.). Furthermore, the most likely benefit provided by the geogrid will be the reduction of routine maintenance over the long-term. Theoretically, the confinement provided by the interlocking of the subballast grains in the geogrid openings will reduce lateral spreading and thus delay the apparition of track misalignments. Therefore, one should not be in a rush to observe a significant and definitive improvement.

Further research on the relationships between these factors is needed, to better understand them and consider them in future analysis.

4 CONCLUSIONS

The installation of this instrumented site has been a success. A preliminary analysis of the measurements, that are currently available, has confirmed that the monitoring system is fully operational and that almost none of the sensors, embedded in the trackbed, were damaged during or after installation.

A closer analysis has revealed that the trackbed is presently behaving as expected despite a few outlying measurements. These outliers can be attributed to the inherent randomness of such a field experiment which is caused by variations in subgrade stiffness, the heterogeneity of the granular materials used as subballast, localized differences during compacting and tamping, dynamic effects induced by fast-moving trains, etc. It is important to reduce noise in our data set by pinpointing the main causes of each abnormality. It would be interesting to instrument another site, presenting similar characteristics, with the same sensors. This would provide a relevant reference, which could be used to determine the impact of some of the aforementioned factors in the quality of the measurements. However, this type of installation is logistically complex and financially onerous so some of the comparisons will have to be approximated using modelling (both physical and numerical).

It is now necessary to carry out a more in-depth analysis of the recordings, which represent approximately 30GB of raw data per month, by applying big data analytics. Thus, our main goal for the future is to refine the automated procedure that has been developed for filtering and signal processing, which will facilitate the required in-depth analysis. Once this step is completed, the various measurements will need to be run through several regression models and correlated with external data in order to identify relevant performance indicators. Studies are underway to determine the best method for conducting the required analysis, and several companion experiments are currently being developed to provide complementary data.

Continued analysis of retained indicators over the next few years should provide enough insight to understand how the geogrids are mobilised when the trackbed is loaded with traffic and to compare the performance of the two geogrids. Over the long-term, this analysis will help SNCF to decide whether the use of geogrids in trackbeds provides enough benefits to warrant their addition to its standards.

5 ACKNOWLEDGEMENTS

The authors would like to acknowledge all the members of the various SNCF teams (DGII-VA-T3, Pôle Régional Ingénierie de Dijon, Infrapôle Bourgogne-Franche-Comté) and Colas Rails, without whom the instrumentation of this site would not have been possible. We would also like to thank the ANRT CIFRE program, which subsidises industrial PhDs such as the one currently conducting this research.

6 REFERENCES

Anantanasakul, P., Indraratna, B., Nimbalkar, S., & Neville, T. (2012). Field monitoring of performance of ballasted rail track with geosynthetic reinforcement. 11th Australia - New Zealand Conference on Geomechanics: Ground Engineering in a Changing World (pp. 241-246). Melbourne: Australian Geomechanics Society and the New Zealand Geotechnical Society.

Carroll, R. (1988). Specifying Geogrids. Geotechnical Fabrics Report, 6(2).

Ellis, G. (2012). Control System Design Guide (Fourth Edition). Sect Appl Princ Control (pp.165–183). doi:10.1016/b978-0-12-385920-4.00009-6. New York, NY: Elsevier.

European Organisation for Technical Approvals. (2017). Non-reinforcing hexagonal geogrid for the stabilization of unbound granular layers by way of interlock with the aggregate, Technical Report TR041, 25p. Brussels.

Fernandes, G., Palmeira, E., & Gomes, R. (2008). Performance of geosynthetic-reinforced alternative sub-ballast material in a railway track. Geosynthetics International, 15(5), 311–321. doi:10.1680/gein.2008.15.5.311

Horníček, L., Břešt'ovský, P., & Jasans, P. (2017). Application of geocomposite placed beneath ballast bed to improve ballast quality and track stability. IOP Conference Series: Materials Science and Engineering, 236(1), pp. 012039. doi:10.1088/1757-899X/236/1/012039.

Lenart, S., & Klompmaker, J. (2014). Geogrid reinforced railway embankment on soft soil – Experiences from 5 years of field monitoring. 10th International Conference on Geosynthetics. Berlin: IGS.

Montgomery, D., & Runger G. (2018). Applied Statistics and Probability for Engineers, 7th Edition. Hoboken, NJ: Wiley.

Nimbalkar, S., & Indraratna, B. (2016). Improved performance of ballasted rail track using geosynthetics and rubber shockmat. Journal of Geotechnical and Geoenvironmental Engineering, 142(8), 04016031-1 - 04016031-13.

Perkins, S. W. (1999). Mechanical response of geosynthetic-reinforced flexible pavements. Geosynthetics International, 6(5), 347-382. https://doi.org/10.1680./gein.6.0157.

Rincent ND Technologies. (2017, Avril). Plaque dynamique légère Manuel d'utilisation, 30p. Courcouronnes, France.

Sharpe, P., Brough, M., & Dixon, J. (2006). Geogrid trials at coppull moor on the west coast main line. Railway Foundations. International Conference on Railway Foundations (pp. 367-375). Railfound 6.

Yaba, O., Emeriault, F., Jenck, O., Ferellec, J.-F., Dhemaied, A. (2020). Suivi In Situ Du Comportement D'une Geogrille Dans Une Plateforme Ferroviaire. 10èmes journées nationales de géotechnique et de géologie de l'ingénieur. Lyon.